17th World Conference on Earthquake Engineering, 17WCEE
Sendai, Japan - September 13th to 18th 2020

INFLUENCE OF HEADED LONGITUDINAL REINFORCEMENT IN GRADE BEAM ON FLEXURAL BEHAVIOR OF COLUMN BASE

N. Onishi[(1)], K. Nishimura[(2)] , Y. Yamaguchi[(3)] , A. Shoji[(3)]

[(1)] *Assistant Professor, The University of Tokyo, onishi@arch.t.u-tokyo.ac.jp*
[(2)] *Associate Professor, Tokyo Institute of Technology, nishimura@m.titech.ac.jp*
[(3)] *Former Graduate Student, Hokkaido University*

Abstract

For exterior beam-column joint, headed reinforcement is now mainly used to avoid the congestion of the bar arrangement. Although beam-column connections including grade beams and column bases in the lowest story are generally designed on condition that hinge yielding at the column bases occurs earlier than the ends of the grade beams, only a few experiments are conducted focusing on the grade-beam-column joint structure that has headed reinforcement for beam longitudinal bars under such yielding condition.

The authors so far experimented with three grade-beam-column-pile exterior joint specimens using headed reinforcement for beam longitudinal bars. The test results showed that the inclined cracks through the head of reinforcement were remarkable on condition that the column yields earlier than the beam. However, these specimens did not satisfy the required development length in the Japanese standards.

This study provides the loading test results of five additional specimens that satisfy the required development length. We focused on the effect of beam anchorage conditions on the bending fracture behavior of columns. Three of the specimens had a single layer of beam longitudinal reinforcement with sufficiently long development length, and the loading test parameters were the amount of column transverse reinforcement and the strength of column longitudinal reinforcement. The others had two layers of longitudinal reinforcement, and the test parameter was the type of anchorage: headed reinforcement and hooked reinforcement. Based on the test result, we concluded as follows:

(1) In the joint with headed reinforcement under cyclic loading, when the top longitudinal reinforcement in the beam has experienced compression force once in the positive-direction loading, in which the beam was loaded toward the column side, the bond stress in the joint will be weak.

(2) The maximum strength increased by about 6% when the column transverse reinforcement ratio raised from 0.21% to 0.48%.

(3) Inclined cracks through the head of bars appeared on the specimens with headed reinforcement for the beam longitudinal reinforcement. The cracks got wider toward the maximum strength. For the specimens with two layers of beam longitudinal reinforcement, the inclined cracks apparently got through the head of the outermost bars.

(4) Cracks along the bent appeared on the specimen with hooked beam reinforcement. Unlike the specimens with headed reinforcement, these cracks did not propagate along inclined cracks across the column. The cracks parallel to the beam tensile bars branched toward the cracks extending along the column tensile bars.

(5) We calculated the column shear forces for two stages: at the yield point of column longitudinal bar and the ultimate state. They can be obtained from the balance of the reaction force at the column support and the forces of longitudinal and transverse reinforcement. The calculation was found to be reasonably accurate in estimating the experimental results.

Keywords: headed reinforcement; column base; grade beam; transverse reinforcement ratio; pile cap

1. Introduction

For exterior beam-column joint, headed reinforcement is now mainly used to avoid the congestion of the bar arrangement. Although beam-column connections including grade beams and column bases in the lowest story are generally designed on condition that hinge yielding at the column bases occurs earlier than the ends of the grade beams, only a few experiments are conducted focusing on the grade-beam-column joint structure that has headed reinforcement for beam longitudinal bars under such yielding condition.

The authors so far experimented with three grade-beam-column-pile exterior joint specimens using headed reinforcement for beam longitudinal bars [1, 2]. The test results showed that the inclined cracks through the head of reinforcement were remarkable on condition that the column yields earlier than the beam. However, these specimens did not satisfy the required development length in the Japanese standards (e.g., AIJ Standard for Structural Calculation of Reinforced Concrete Structures revised 2010 [3]).

This study provides the loading test results of five additional specimens that satisfy the required development length. We focused on the effect of beam anchorage conditions on the bending fracture behavior of columns. Three of the specimens had a single layer of beam longitudinal reinforcement with sufficiently long development length, and the loading test parameters were the amount of column transverse reinforcement and the strength of column longitudinal reinforcement. The others had two layers of longitudinal reinforcement, and the test parameter was the type of anchorage: headed reinforcement and hooked reinforcement.

2. Test Program

Cyclic loading tests of five specimens are conducted. This chapter outlines features of the specimens, the loading program, instrumentations of measurement, and calculated strengths.

2.1 Specimens

All five specimens were on a 1/3-scale including an exterior column, a grade beam, and a single pile. Specimen details are shown in Fig. 1. The beam section was 250 mm wide and 600 mm deep. The column had a 300 mm wide square section whereas the pile had a 400 mm wide square section. The horizontal cross-sectional dimensions of the pile cap were 500 mm by 500 mm, and its height was 450 mm. Table 1 lists the concrete cylinder test results. Table 2 lists the tensile test results of the steel bars. In this work, the hatched area illustrated in Fig. 1 was defined as the “joint region.”

The longitudinal reinforcement was 8 D13 (SD295A or SD390) in the column, 12 D13 (SD295A) in the pile, 5 D16 (SD295A) in the single-layered beam, and 8 D13 (SD295A) in the double-layered beam. The deformed bars complied with the Japanese Industrial Standard (JIS G 3112). Four specimens use “mechanical anchorages” (Tokyo Tekko), so-called headed reinforcement bars, for beam longitudinal reinforcement.

To simplify discussions of member performances and internal joint stress transfer, the shape of the horizontal cross-section of the pile was square, and all members including the pile had a single layer bar arrangement.

Specimens No.1–No.3 have single-layered beam, whereas specimens No.4 and No.5 have double-layered beam. Specimen No.2 uses SD390 for the column longitudinal bars, whereas the other specimens use SD295A. The column transverse reinforcement ratio of No.3 is 0.48% using D10 (SD295A), whereas that of the other specimens is 0.21% using D6 (SD295A). Specimen No.5 has hooked anchorages. The development lengths of specimens No.1–No.4 and that of the outermost bars of No.5 are 240 mm for column side, and 290 mm for pile side, measured from column face and pile face, respectively. The development lengths of the second layer of No.5 are 200 mm for column side, and 250 mm for pile side.

2.2 Loading Program

Fig. 2 illustrates the loading apparatus used in the tests. The column and pile were supported and the tip of

the pile was connected to a reaction beam. The beam of a specimen was cyclically loaded by a hydraulic jack. For all the specimens, the beam was initially loaded toward the column side, which is defined as "positive loading." Loading the beam toward the pile side is defined as "negative loading." Loading was controlled by the displacement of the loading point. Lateral loading history consisted of several sets of cycles. The target drift ratio of each loading set was ±0.25%, ±0.5%, ±0.75%, ±1%, ±1.5%, ±2%, and ±3%. Loading sets of ±0.5% or more drift had two cycles each. For specimen No.3, ±4% drift set was added. After these loading sets, specimens were loaded until −5% drift.

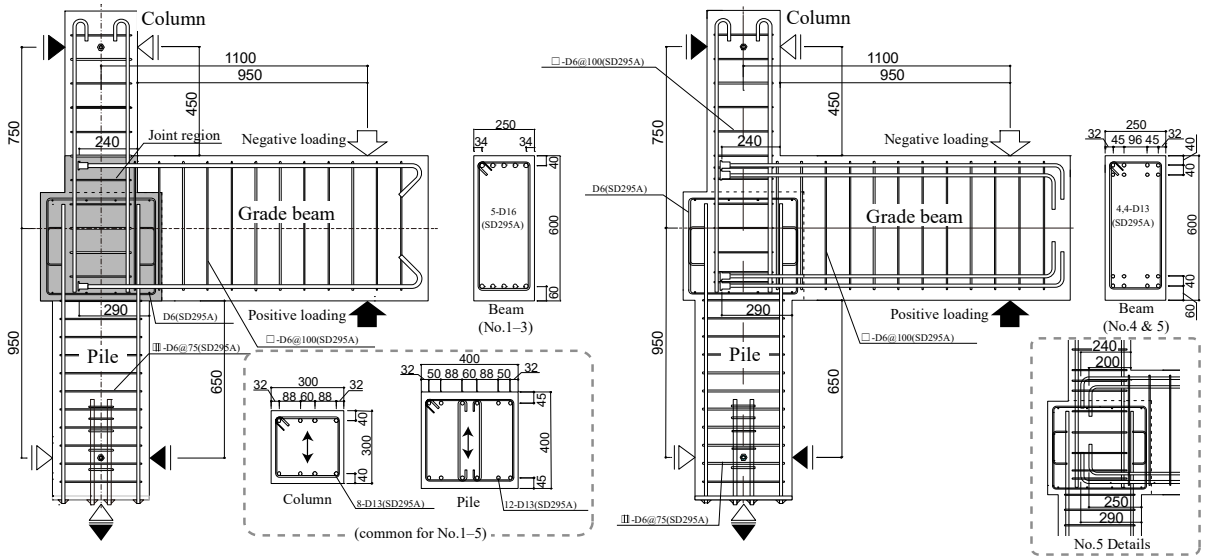

Figure 1. Specimen details.

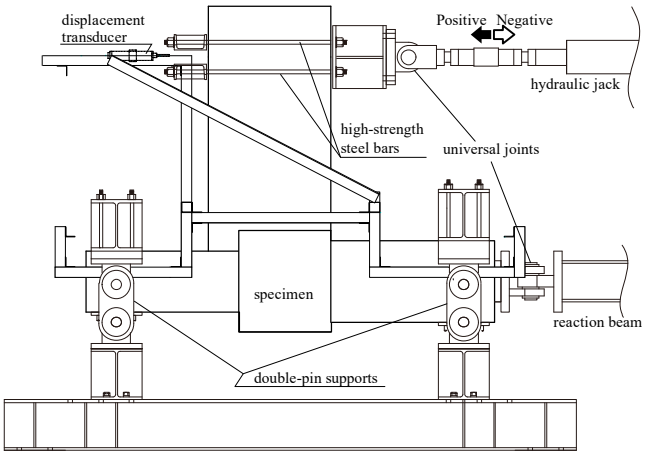

Figure 2. Loading apparatus and measurement frame.

Table 1. Concrete cylinder test results.

Name	Compressive strength σ_B (MPa)	Tensile strength σ_t (MPa)	Young's modulus E_c (GPa)
No.1	37.0	2.8	25.8
No.2	37.9	2.7	25.8
No.3	37.8	2.7	25.3
No.4	35.3	2.3	23.4
No.5	36.2	2.6	23.3

Table 2. Steel bar tensile test results.

Use	Diameter (Standard)	Yield strength σ_y (MPa)	Tensile strength σ_m (MPa)	Young's modulus E_s (GPa)
Beam	D16 (SD295A)	351	515	195
	D13 (SD295A)	354	504	194
Column	D13 (SD295A)	338	481	192
	D13 (SD390)	426	581	197
Transverse reinforcement	D6 (SD295A)	392*	550	200
	D10 (SD295A)	352	512	193

*0.2% proof stress

2.3 Instrumentation of measurement

Displacement transducers were placed on the steel frames as shown in Fig. 2. The drift ratio was defined as the beam-tip displacement divided by the length from the beam-tip to the axis of column.

Fig. 3 shows the position of strain gauges. The gauges on the longitudinal reinforcement were placed on the lines that main cracks might be observed. The other gauges on the transverse reinforcement were placed on the axis of the column and pile. The strain gauges were placed in the half part of each specimen, considering the symmetry of specimens.

2.4 Calculated Strength

Table 3 lists the calculated strength of members on two stages: the yield point of longitudinal bars ("Yield state") and the ultimate state ("Ultimate state"). These strengths were determined by cross-section analysis using measured material properties (Table 1 and 2). "Shear force of beam" in this table is the smallest of three shear forces of the beam converted from the bending moment of the column, beam, and pile.

The stress–strain curve of compressive concrete followed a modified Kent–Park model [4], and the tensile

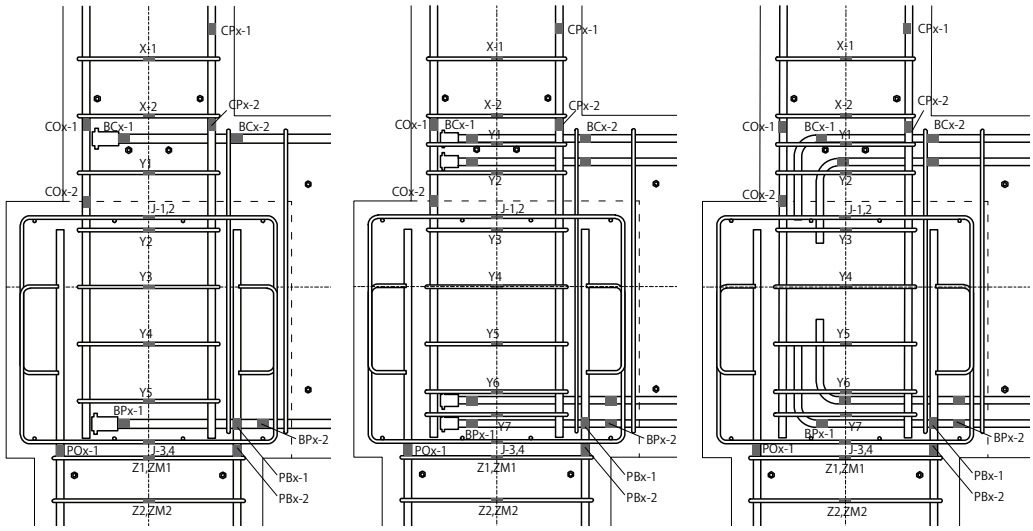

(a) No.1–3 (b) No.4 (c) No.5

Figure 3. Position of strain gauges.

Table 3. Calculated flexural strength of each member and shear force of beam at yield and ultimate state.

Specimen	Loading direction	Yield moment (kNm)			Ultimate moment (kNm)			Shear force of beam (kN)		Critical member	Column-to-beam strength ratio**
		Column	Pile*	Beam	Column	Pile*	Beam	Yield state	Ultimate state		
No.1	+	41	60	174	45	67	181	140	155	Column	0.81
	−	−41	−109	−179	−45	−117	−189	−140	−155	Column	0.69
No.2	+	51	60	174	55	67	181	144	158	Pile	0.83
	−	−51	−114	−179	−55	−123	−189	−176	−190	Column	0.85
No.3	+	41	60	174	45	67	181	140	156	Column	0.82
	−	−41	−109	−179	−45	−118	−189	−140	−156	Column	0.70
No.4	+	41	60	162	45	67	184	140	154	Column	0.80
	−	−41	−108	−168	−45	−117	−193	−140	−154	Column	0.68
No.5	+	41	60	163	45	67	184	140	154	Column	0.80
	−	−41	−109	−169	−45	−117	−194	−140	−154	Column	0.68

* Axial force at the ultimate state of column was applied as a result of iteration.
** Ratio of the smallest ultimate moments of the column and pile to the ultimate moment of the beam.

steel was treated as an elastic–perfectly plastic material. During the tests of specimens, steel bars unreached the strain hardening level.

When converting moment to shear force of the beam, critical sections are assumed as follows: for the column, the top surface of the beam; for the pile, the bottom surface of the beam; for the beam under positive loading, the column face; and for the beam under negative loading, the pile-cap face.

3. Test Results

3.1 Relationship between Beam Shear Force and Drift Ratio

Fig. 4 shows the relationship between beam shear force, Q_b, and drift ratio, R. In this graph, Q_y and Q_u represent calculated strengths shown in Table 3. CY and PY respectively represent the yield point of longitudinal bars in the column and pile. Because dimensions of all specimens were the same, specimens showed almost the same initial stiffness. The yield points of the column and pile, which are determined from measured material properties, and the maximum shear forces were observed as follows.

(1) Specimen No.1

Column longitudinal bars yielded when R = +0.5% (+2 Cycle) and R = −0.5% (−2 Cycle). Then they yielded at the upper face of the pile cap (+6 Cycle peak). The maximum shear forces were Q_b = 153 kN (+8 Cycle peak) and Q_b = −142 kN (during the cycle of pushing over toward R = −5%).

(2) Specimen No.2

Column longitudinal bars yielded when R = +1.5% (+8 Cycle) and R = −0.75% (−4 Cycle). Pile longitudinal bars yielded when R = +0.5% (+2 Cycle). The maximum shear forces were Q_b = 167 kN (+10 Cycle peak) and Q_b = −170 kN (−8 Cycle peak).

(3) Specimen No.3

Column longitudinal bars yielded when R = +0.5% (+2 Cycle) and R = −0.5% (−2 Cycle). Then they yielded at the upper face of the pile cap (+5 Cycle). The maximum shear forces were Q_b = 164 kN (+12 Cycle peak) and Q_b = −150 kN (during the cycle of pushing over toward R = −5%).

(4) Specimen No.4

Column longitudinal bars yielded when R = +0.5% (+2 Cycle) and R = −0.5% (−2 Cycle). Pile longitudinal

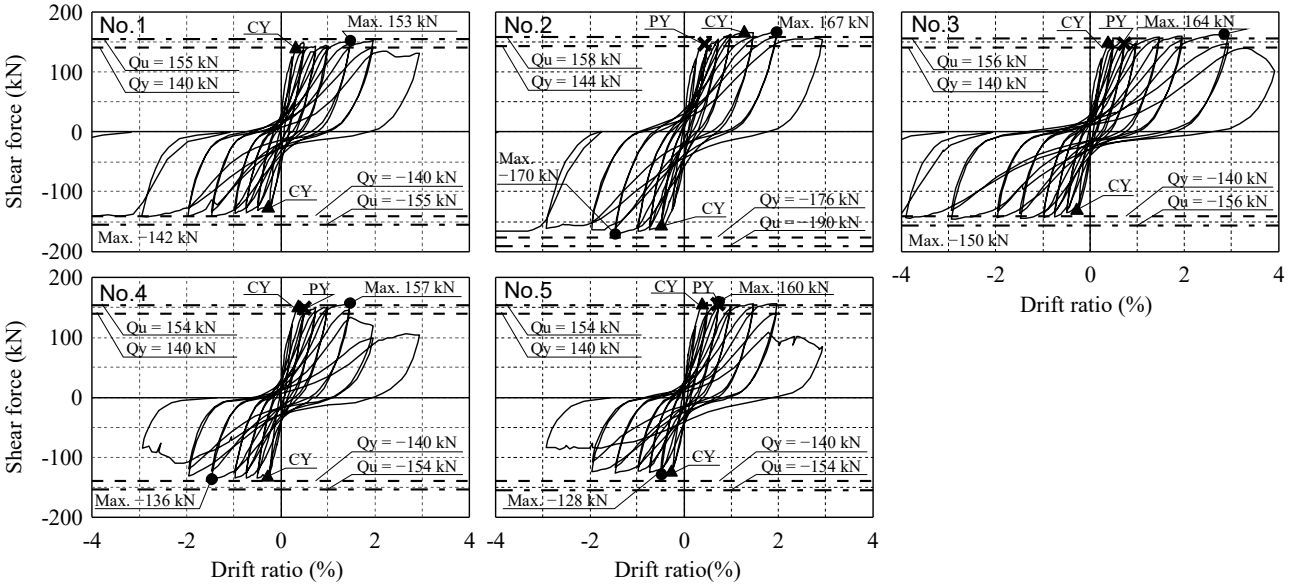

Figure 4. Relationship between beam shear force and drift ratio.

bars yielded when R = +0.5% (+2 Cycle). The maximum shear forces were Q_b = 157 kN (+8 Cycle) and Q_b = −136 kN (−8 Cycle).

(5) Specimen No.5

Column longitudinal bars yielded when R = +0.5% (+2 Cycle) and R = −0.5% (−2 Cycle). Pile longitudinal bars yielded when R = +0.75% (+4 Cycle). The maximum shear forces were Q_b = 160 kN (+4 Cycle) and Q_b = −128 kN (−2 Cycle).

3.2 Crack Patterns

Fig. 5 shows crack patterns at the cycle peak when the maximum beam shear force reached during negative loading and Fig. 6 shows photographs at the end of the loading tests. Flexural cracks were observed in the column, beam, and pile by 0.25% drift except the pile of specimen No.3 under negative loading. Inclined cracks were observed in the column and beam by 0.75% drift. Cracks on the pile cap were observed by 0.5% to 0.75% drift.

Inclined cracks through the head of bars appeared on the specimens with headed reinforcement for the beam longitudinal reinforcement. The cracks got wider toward the maximum strength. For the specimens with two layers of beam longitudinal reinforcement, the inclined cracks seemingly got through the head of the outermost bars.

Cracks along the bent appeared on the specimen with hooked beam reinforcement. Unlike the specimens with headed reinforcement, these cracks did not propagate along inclined cracks across the column. The cracks parallel to the beam tensile bars branched toward the cracks extending along the column tensile bars.

3.3 Strains of Transverse Reinforcement

Fig. 7 shows distributions of transverse reinforcement strain data of the gauges X1–X2, Y1–Y7, and Z1–Z2. The strain gauges located near inclined cracks demonstrate that the transverse reinforcement yielded by the

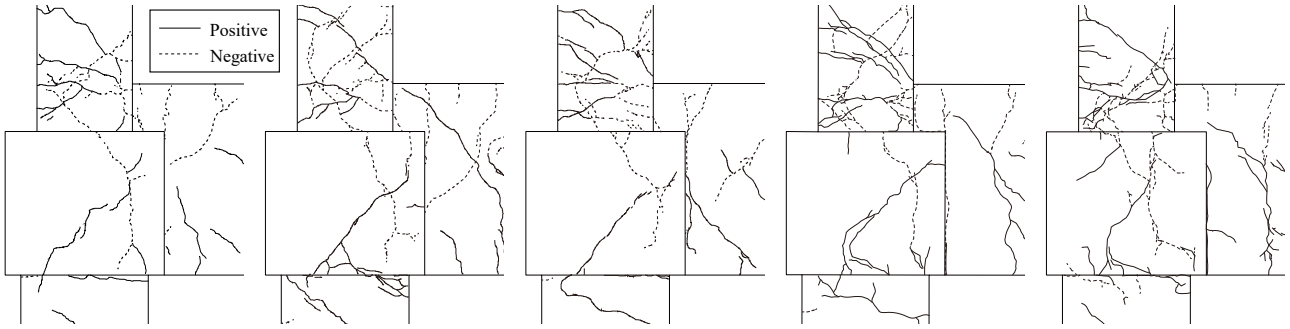

(a) No.1 (b) No.2 (c) No.3 (d) No.4 (e) No.5

Figure 5. Crack patterns (R = 1.5%).

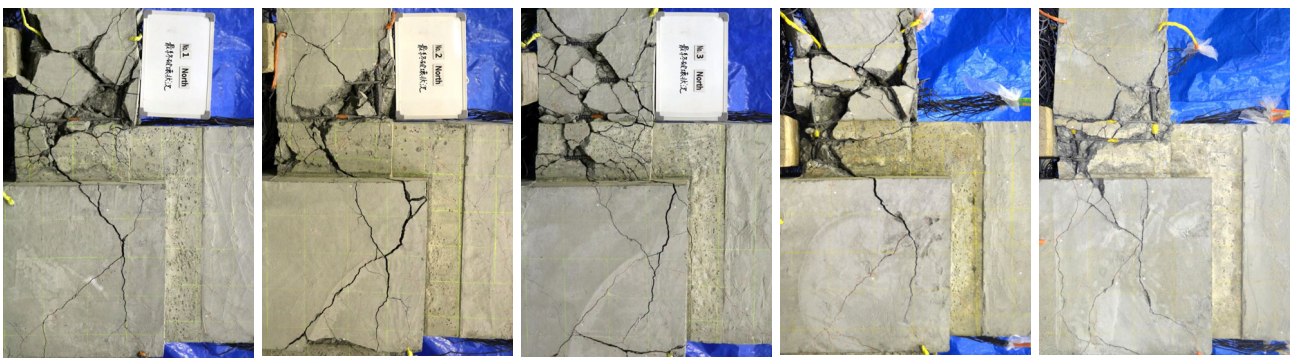

(a) No.1 (b) No.2 (c) No.3 (d) No.4 (e) No.5

Figure 6. Photographs at the end of the loading tests

drift of 2.0%.

3.4 Strains of Beam Longitudinal Reinforcement

Fig. 8 shows the time history of strains of beam longitudinal reinforcement. Data of specimen No.1 to No.3 are plotted. Solid lines are strains at 50 mm to the head of the beam bars and dashed lines are strains at the column face.

Transferring tension of longitudinal bars to concrete via bond stress around tensile bars would allow the end of beam bars to have less strain than the bars at the column face. However, the test results showed the strains at these positions had almost the same value during negative loading.

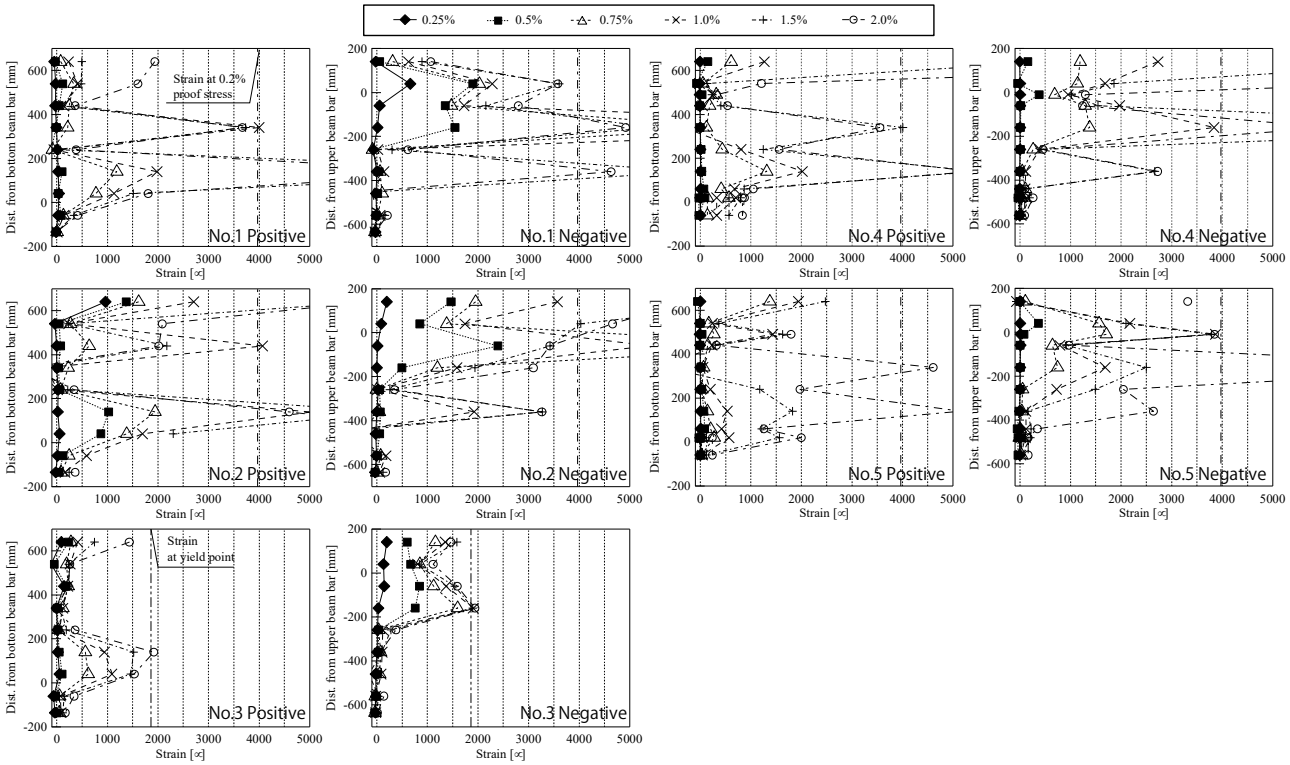

Figure 7. Distribution of transverse reinforcement strains.

4. Discussion

4.1 Flexural Capacity of Specimens

Column longitudinal bars of all the specimens excluding No.2 yielded in the cycle of $R = \pm 0.5\%$. For specimen No.2, because the strength of the column longitudinal bars is higher than those of the other specimens, the drift ratio of column yield point was larger than 0.5%, and the capacity of the specimen in positive loading results from the yielding of pile longitudinal bars.

During positive loading, all the specimens excluding specimen No.1 had a maximum capacity greater than the calculated ultimate strength, and specimen No.1 showed a maximum capacity nearly equal to the calculated value. They showed the capacity by 1.5% drift.

During negative loading, the maximum capacity of all the specimens did not reach the calculated ultimate strength, even though the column longitudinal bars yielded. We will discuss this further in section 4.4.

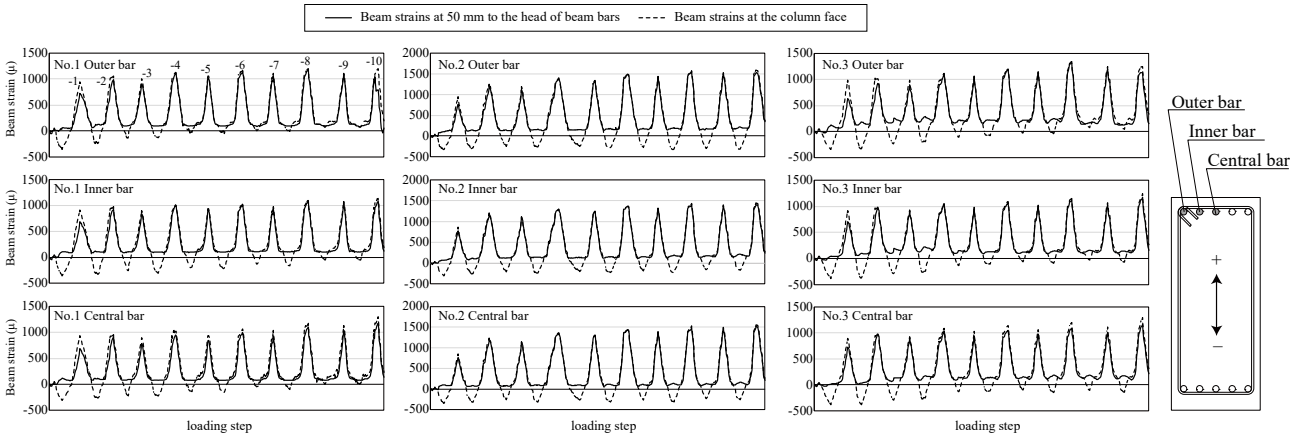

Figure 8. History of beam longitudinal bar strains.

4.2 Bond Stress on Beam Longitudinal Bars

This section discusses the accordance of the beam strains at the column face and the end of the beam bars. Test results indicated cracks as follows: (1) in positive loading, flexural cracks of the column in the extension of the beam upper surface and those of the beam-column joint outside the pile cap, (2) in negative loading, inclined cracks running across the beam-column joint outside the pile cap. These cracks gradually widened as the drift increased.

Internal damage of concrete around beam longitudinal bars that occurred in positive loading can weaken the bond stress of the straight portion in negative loading; therefore, the head of beams would have supported most tensile force of beam longitudinal bars in negative loading.

4.3 Effect of Column Transverse Reinforcement

The maximum strengths of specimen No.1 were Q_b = 153 kN (+8 Cycle peak) and Q_b = −142 kN (during the cycle of pushing over toward R = −5%), and those of specimen No.3 were Q_b = 164 kN (+12 Cycle peak) and Q_b = −150 kN (during the cycle of pushing over toward R = −5%). The maximum strength increased by 7.1% for positive loading and 5.6% for negative loading when the column transverse reinforcement ratio raised from 0.21% to 0.48%.

4.4 Strength Estimation in Negative Loading

This section discusses the flexural behavior of specimens in negative loading with previously developed model [1, 2].

4.4.1 Mainly observed cracks

Fig. 9 illustrates an example of observed main cracks. Specimens No.1 through No.4 shows inclined cracks apparently running across the head of longitudinal reinforcement. These inclined cracks gradually widened as the drift increased. The crack pattern of these specimens was seemingly similar to that of the specimens tested previously by Onishi et al. (2018) [1]. We applied the model to specimen No.1 through No.4 and compared them with the test results.

4.4.2 A Model for Specimens with Long Development Length

This section outlines the previously developed model for specimens with long development length (Fig. 10). This calculation is based on the equilibrium of moments on a free body of the column. This requires forces of longitudinal and transverse reinforcement across an assumed 45-degree crack line. For specimen No.4, the 45-degree crack line was assumed to run through the end of the outermost beam longitudinal bars.

The estimated capacities at yield and ultimate states were calculated based on the following definitions. The yield state was defined as when the tensile force of column longitudinal bars, T_s, reaches the yield strength.

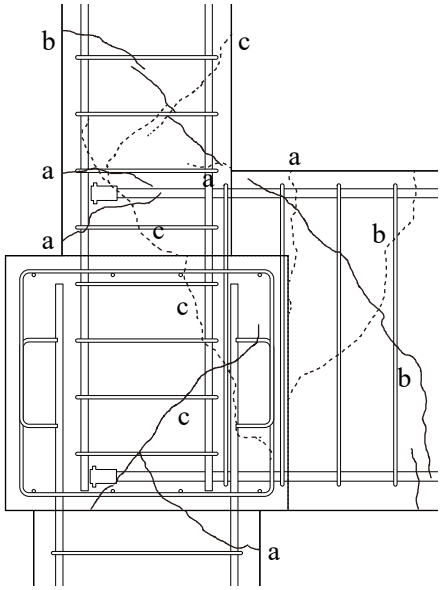

Figure 9. An example of main cracks (specimen No.2).

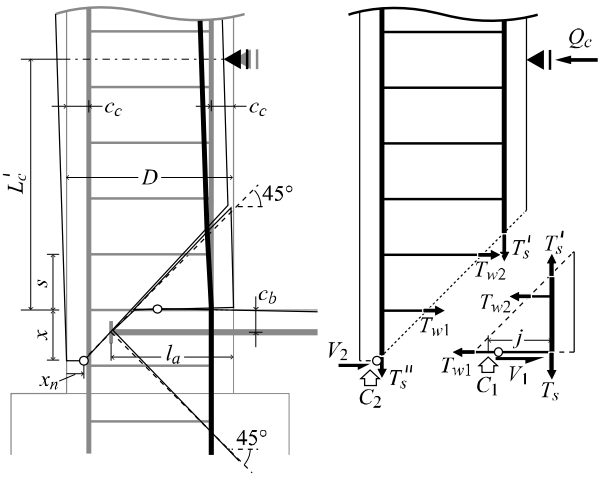

Figure 10. Capacity model for specimens with long development length.

The ultimate state was defined as when the compression face strain reaches the ultimate strain (=0.3%) using the stress block method.

4.4.3 Comparison with Test Results

We calculated the column shear forces for two stages: at the yield point of column longitudinal bar and the ultimate state. Fig. 11 plots the beam shear forces converted from the calculated column shear forces. The forces were calculated with the previously developed model. The calculation was executed only for specimens No.1–No.4, because the crack pattern of specimen No.5 seemingly unfitted the assumed inclined crack line of the capacity model.

The estimated ultimate capacity obtained with the model was compared with the maximum capacity resulted from the loading tests. The estimated capacities at yield and ultimate states estimated the yield and maximum strength within a tolerance of five percent. The calculation was found to be reasonably accurate in estimating the experimental results.

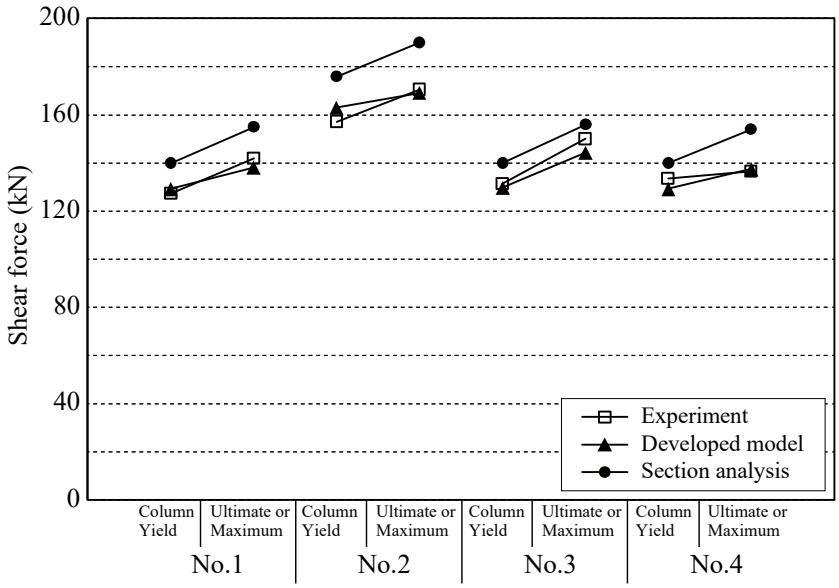

Figure 11. Comparison with calculated values and experimental values.

5. Conclusion

Based on the test result, we concluded as follows:

(1) In the joint with headed reinforcement under cyclic loading, when the top longitudinal reinforcement in the beam has experienced compression force once in the positive-direction loading, in which the beam was loaded toward the column side, the bond stress in the joint will be weak.

(2) The maximum strength increased by about 6% when the column transverse reinforcement ratio raised from 0.21% to 0.48%.

(3) Inclined cracks through the head of bars appeared on the specimens with headed reinforcement for the beam longitudinal reinforcement. The cracks got wider toward the maximum strength. For the specimens with two layers of beam longitudinal reinforcement, the inclined cracks apparently got through the head of the outermost bars.

(4) Cracks along the bent appeared on the specimen with hooked beam reinforcement. Unlike the specimens with headed reinforcement, these cracks did not propagate along inclined cracks across the column. The cracks parallel to the beam tensile bars branched toward the cracks extending along the column tensile bars.

(5) We calculated the column shear forces for two stages: at the yield point of column longitudinal bar and the ultimate state. They can be obtained from the balance of the reaction force at the column support and the forces of longitudinal and transverse reinforcement. The calculation was found to be reasonably accurate in estimating the experimental results.

6. Acknowledgments

This research was supported by JSPS KAKENHI Grant Number 16K18179.

7. References

[1] Onishi N, Nishimura K, Yamaguchi Y (2018): Effects of development length of beam bars and shear reinforcement ratio of column on exterior foundation beam-column joint with mechanical anchorage at beam bar ends, *J. Struct. Constr. Eng.*, AIJ, **83** (743), 167–177. (in Japanese)

[2] Onishi N, Nishimura K (2018): Loading test of exterior footing beam-column joint with mechanically anchored beam bars, *Proceedings of the 11th National Conference on Earthquake Engineering*, Earthquake Engineering Research Institute, Los Angeles, CA.

[3] Architectural Institute of Japan (2019): *AIJ Standard for Structural Calculation of Reinforced Concrete Structures*, revised 2010.

[4] Park R, Priestley MJN, Gill WD (1982): Ductility of square confined concrete columns, *Journal of the Structural Division ASCE*, **108** (4), 929–950.

